PHYSICAL REVIEW E **105**, 054608 (2022)

Simple two-dimensional models of alcohols

Petra Papez
Laboratory for Molecular Modeling, National Institute of Chemistry, Hajdrihova 19, SI-1001, Slovenia
and Department of Physics, Faculty of Mathematics and Physics, University of Ljubljana, Jadranska 19, SI-1000, Slovenia

Tomaz Urbic
Faculty of Chemistry and Chemical Technology, University of Ljubljana, Vecna Pot 113, SI-1000 Ljubljana, Slovenia

(Received 18 February 2022; accepted 11 May 2022; published 27 May 2022)

Alcohols are organic compounds characterized by one or more hydroxyl groups attached to a carbon atom of an alkyl group. They can be considered as organic derivatives of water in which one of the hydrogen atoms is replaced by an alkyl group. In this work, the Mercedes-Benz model of water is used to design simple two-dimensional (2D) models of lower alcohols. The structural and thermodynamic properties of the constructed simple models are studied by conducting Monte Carlo simulations in the isothermal-isobaric ensemble. We show that 2D models display similar trends in structuring and thermodynamics as in experiments. The present work on the smallest amphiphilc organic solutes provides a simple testing ground to study the competition between polar and non-polar effects within the molecule and physical properties.

DOI: 10.1103/PhysRevE.105.054608

I. INTRODUCTION

We hardly imagine life without water. Liquid water covers approx. 75% of Earth's surface and represents approx. 60–75% of human body weight. Furthermore, in living organisms it has an important role as a solvent, temperature buffer, and metabolite. The water molecule is a simple molecule composed of two hydrogen atoms and one oxygen atom. It is well known of its anomalous properties, which result from a strong orientation-dependent hydrogen bonding and strong intermolecular associations and enable life to exist. In addition, alcohols can be considered as the organic derivatives of water with amphiphilic properties. Their hydroxyl group represents the polar part and can form hydrogen bonds (HBs) with other water and alcohol molecules in the vicinity. Moreover, it contributes to the solubility of an alcohol in water. In contrast, their alkyl chain represents the non-polar part. Although that lower alcohols, i.e., methanol, ethanol, propan-1-ol, isopropyl alcohol, and even *t*-butanol, are miscible with water in all proportions, this does not apply to higher alcohols, because of the greater non-polar parts. As the simplest alcohol, methanol differs from water in the presence of a methyl group. Compared to the water molecule, methanol has only one donor and one or two HB acceptor sites [1]. While its methyl group contributes to some of methanol's unusual properties, e.g., the minimum in partial molar volume, and to the maintenance of the water structure in its vicinity, the hydroxyl group contributes to its solubility in water. The properties of its condensed phase highly depend on the HB formation [2,3]. For this reason, methanol represents a suitable model system for studying solvation in aqueous mixtures and the formation of HBs [4]. In 1960 Pauling [5] assumed that hexameric ring-shaped structures of methanol molecules predominate in the liquid phase. Nevertheless, today it is believed that molecules in its liquid phase form clusters and chains, but hitherto the distribution of cluster sizes is not well defined [6,7]. In experimental study, Sarkar *et al.* [8] showed the presence of clusters assembled of six methanol molecules. Similarly, based on the computational and experimental results, Kashtanov *et al.* [7] suggested that liquid methanol consists of rings and chains formed of six to eight methanol molecules. On the other hand, using Raman spectroscopy, Lin *et al.* [6] examined the microscopic structure of liquid methanol, where ring structures assembled of three methanol molecules and chains formed of three, four, and five molecules were found to predominate. In addition, they also observed the temperature dependence of the cluster size distribution. Besides, Yamaguchi *et al.* [9] showed that the chain in liquid methanol consists of an average of 2.7 methanol molecules and that an average of 1.3 HBs are formed per methanol molecule [10]. Chains were also found to be nonlinear on average (due to steric effects [7]). The next in a row is ethanol. In its liquid phase, the presence of hexameric clusters, closed tetramers, and U-shaped tetramers was suggested by Sarkar and Joarder [11]. Similar was also proposed by Benmore and Loh [12]. By performing molecular dynamics simulations, Saiz *et al.* [13] showed that the majority of molecules form two HBs and that the liquid ethanol consists mostly of linear chains linked by HBs. Furthermore, the temperature was found to affect the length of a chain. While at higher temperatures monomers predominate, at lower temperatures longer chains are found. Ethanol is followed by propan-1-ol and *t*-butanol with even more pronounced non-polar parts. Experimental study on cluster formation in propan-1-ol was made by Takamuku *et al.* [14] while Sum and Sandler [15] in their theoretical study also focused on cooperativity in

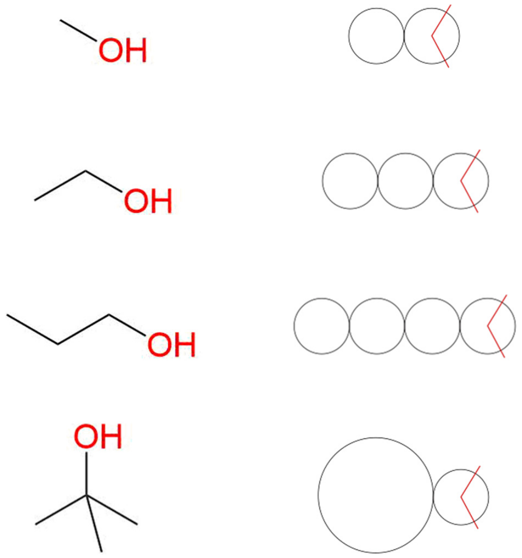

FIG. 1. Skeletal representations of lower alcohols under consideration and their proposed 2D models.

the cluster formation among lower alcohols, i.e., methanol, ethanol, and propan-1-ol. Less is known about *t*-butanol. The intermolecular structure of liquid *t*-butanol was investigated by Narten and Sandler [16] and also by Bowron *et al.* [17].

Both water and alcohols are commonly inspected by experimental techniques (e.g., x-ray and neutron diffraction and by Raman spectroscopy) and computer simulations [e.g., Monte Carlo (MC) and molecular dynamics simulations and by density functional theory calculations]. Accordingly, models of different complexity have been developed to model structural and thermodynamic properties of water and alcohols. For instance, water can be modelled using computational expensive atomistic models, which aim to incorporate realistic details and therefore include variables describing van der Waals and Coulomb interactions, hydrogen bonding, etc. [18–21]. However, many properties of water and its solutions can be described by computational less expensive simple models [22–24]. One of the simplest models, the so-called Mercedes-Benz (MB) model, was proposed by Ben-Naim in 1971 [25]. In this model, interaction between two particles is a superposition of two functions, i.e., one of the Lennard-Jones (LJ) type, depending only on the intermolecular distance, and a HB potential, which depends on the distance between two particles and on their relative orientation. The water molecule is modelled as a two-dimensional (2D) spherical disk with three symmetrically arranged arms that mimic the formation of HBs and are separated by a fixed angle of 120°,

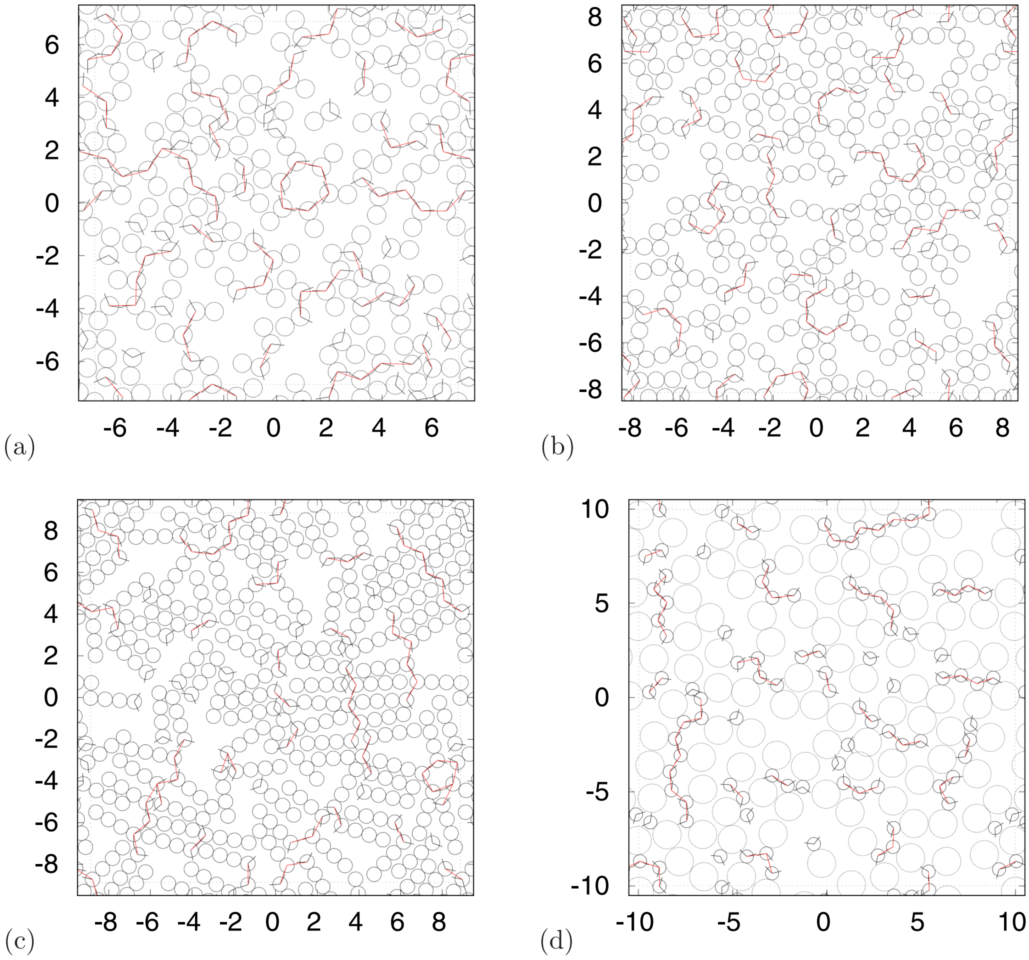

FIG. 2. Snapshots of (a) methanol-, (b) ethanol-, (c) propan-1-ol-, and (d) *t*-butanol-like system at temperature 0.16.

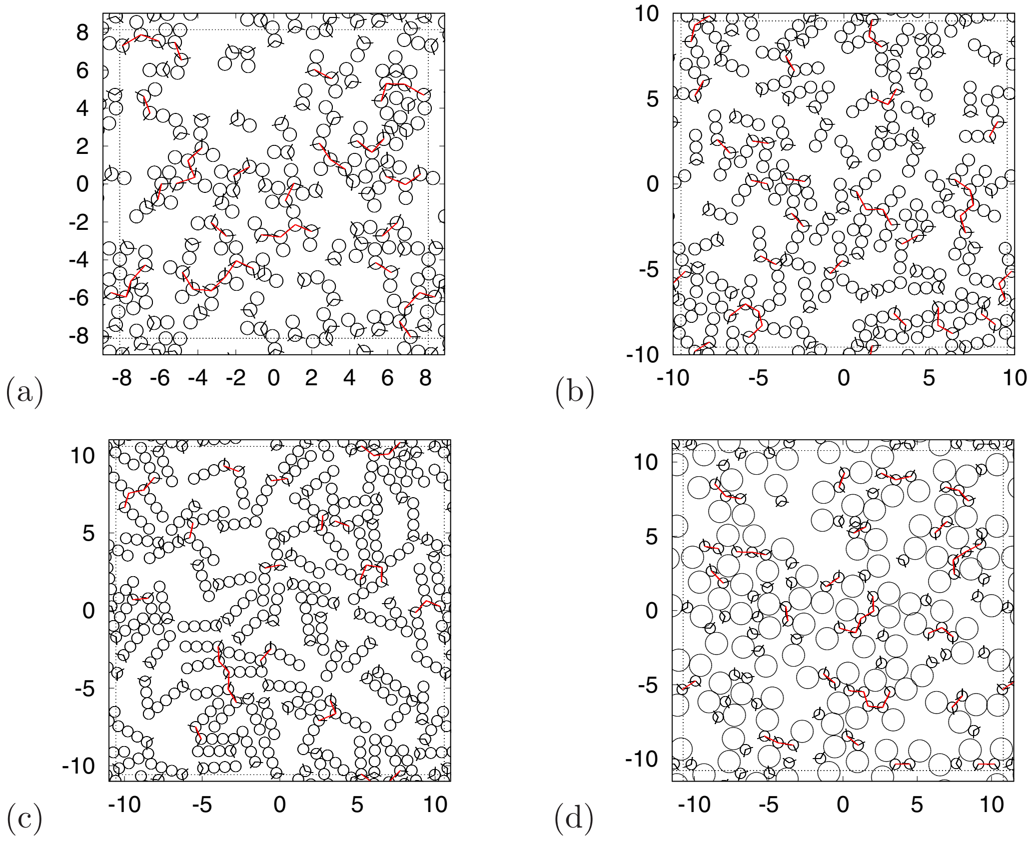

FIG. 3. Same as in Fig. 2 and at temperature 0.24.

as in the MB logo. The strongest HB occurs when an arm of one particle is co-linear with the arm of another particle and when two arms are pointing in the opposite directions [23]. The major advantage of simple 2D models is that they provide greater computational efficiency. For such models, thermodynamic properties can be computed with computer simulations in a reasonable amount of time. Moreover, the underling physical principles can be thus more extensively explored and also visualized in 2D. It was previously shown by MC simulations in the isothermal-isobaric (NPT) ensemble that the MB model successfully qualitatively predicts the density anomaly, the minimum in isothermal compressibility as a function of temperature, large heat capacity, and also different thermodynamic properties of solvation of non-polar solutes [26–32]. Analytical methods such as thermodynamic perturbation theory, integral equation theory, and statistical mechanical modeling were also used to study 2D MB model [33–43]. Recently, the effect of rotational and translational degrees of freedom on structural and thermodynamic properties of the system were studied by integral equation theory, thermodynamic perturbation theory and MC simulations [44–47]. The 2D MB like methanol was introduced before by Hribar-Lee and Dill [48] and Primorac *et al.* [49]. Alcohol particles were modelled as 2D LJ disks with two arms separated by an angle of 120° (as in the MB model), and for each C atom in the alcohol molecule, another LJ disk of the same size was added into the molecule in the direction of a "missing" HB. In the Hribar-Lee and Dill [48] model, the disks were overlapped, while in the model of Primorac *et al.* [49] the disks were tangential. Hribar-Lee and Dill studied the alcohol-water mixtures, whereas Primorac *et al.* compared both models.

In this study we construct more alcohol-like particles in the same manner as proposed by Primorac *et al.* [49]. We investigate the structural and thermodynamic properties exhibited by simple models of lower alcohols, i.e., methanol, ethanol, propan-1-ol, and *t*-butanol, by conducting the NPT MC simulations. We aim to address the questions of HB formation and cluster size distribution in systems of particles with alcohol-like properties and compute thermodynamic properties as functions of temperature and compare them with the experimentally obtained data of the corresponding alcohols. From now on, the paper is organized as follows. In Sec. II, the MB models of alcohols are presented. The computational details are provided in Sec. III. Next, in Sec. IV, the discussion of the obtained structural and thermodynamic results is made. In Sec. V we summarize some of the main results and conclude the paper.

II. THE MODELS

Four different models with alcohol-like properties are represented as the extended 2D MD model of water (see Fig. 1). Alcohols are modelled as dimers, trimers, or tetramers of disks at a fixed separation. First disk, named site 0, represents hydroxyl group which interacts also with other hydroxyl groups through orientational dependent HB interaction and with all non-polar sites, named 1 (2 or 3) through LJ interaction. Second (third or fourth) disk, named site 1 (2 or 3), represents the non-polar group which can with all other non-polar sites interact through LJ interaction. The energy of interaction between two particles $U(\mathbf{R_i},\mathbf{R_j})$ is defined as the sum of the LJ potential ($U_{\rm LJ}$) and HB interaction ($U_{\rm HB}$):

$$U(\mathbf{R_i},\mathbf{X_i},\mathbf{R_j},\mathbf{X_j}) = \sum_{\alpha,\beta=0}^{1(2,3)} U^{\rm LJ}_{\alpha\beta}(|\mathbf{r_{i\alpha}}-\mathbf{r_{j\beta}}|) + U_{\rm HB}(\mathbf{r_{i1}},\mathbf{X_i},\mathbf{r_{j1}},\mathbf{X_j}), \qquad (1)$$

where $\mathbf{R_i}$ and $\mathbf{R_j}$ are position vectors of centers of mass of particles i and j, respectively. $\mathbf{X_i}$ and $\mathbf{X_j}$ are orientational vectors. $\mathbf{r_{i\alpha}}$ is a position vector of site α in particle i and $\mathbf{r_{j\beta}}$ is a position vector of site β in particle j, respectively. The sum over α and β in Eq. (1) goes from 0 to 1 in the case of methanol and t-butanol, from 0 to 2 in the case of ethanol, and from 0 to 3 in the case of propan-1-ol. The LJ term is calculated using the standard formula

$$U^{\rm LJ}_{\alpha\beta}(r) = 4\varepsilon^{\rm LJ}_{\alpha\beta}\left[\left(\frac{\sigma^{\rm LJ}_{\alpha\beta}}{r}\right)^{12} - \left(\frac{\sigma^{\rm LJ}_{\alpha\beta}}{r}\right)^{6}\right]. \qquad (2)$$

Here, $\varepsilon^{\rm LJ}_{\alpha\beta}$ and $\sigma^{\rm LJ}_{\alpha\beta}$ are the well-depth and contact parameter, respectively. The parameters for dissimilar segments are obtained from the Lorentz-Berthelot combining rules. Hydroxyl groups are represented as 2D LJ disks with two arms separated by an angle of 120°. Hydroxyl groups form HBs with an energy, which is a Gaussian function of separation and angle:

$$U_{\rm HB}(\mathbf{r_{i1}},\mathbf{X_i},\mathbf{r_{j1}},\mathbf{X_j}) = \sum_{k,l=1}^{2} U^{kl}_{\rm HB}(|\mathbf{r_{i\alpha}}-\mathbf{r_{j\beta}}|,\theta_i,\theta_j). \qquad (3)$$

$U^{kl}_{\rm HB}$ stands for the energy of interaction between two arms of different particles:

$$U^{kl}_{\rm HB}(r_{ij},\theta_i,\theta_j) = \varepsilon_{\rm HB}G(r_{ij}-r_{\rm HB})G(\vec{i}_k\vec{u}_{ij}-1)G(\vec{j}_l\vec{u}_{ij}+1), \qquad (4)$$

$$U^{kl}_{\rm HB}(r_{ij},\theta_i,\theta_j) = \varepsilon_{HB}G(r_{ij}-r_{\rm HB})G\left(\cos\left(\theta_i+\frac{2\pi}{3}k\right)-1\right) \times G\left(\cos\left(\theta_j+\frac{2\pi}{3}l\right)+1\right), \qquad (5)$$

where $G(x)$ is an unnormalized Gaussian function

$$G(x) = \exp\left(-\frac{x^2}{2\sigma^2}\right). \qquad (6)$$

The unit vectors $\vec{i}_k$ and $\vec{j}_l$ represent the k^{th} arm of the i^{th} particle and the l^{th} arm of the j^{th} particle ($k,l=1,2$), respectively, while $\vec{u}_{ij}$ stands for the unit vector joining the center of particle i to the center of particle j. θ_i and θ_j are the orientations of particle i and j, respectively. The parameters $\varepsilon_{\rm HB}=-1$ and $r_{\rm HB}=1$ define optimal HB energy and bond length, respectively. The same width parameter $\sigma_{\rm HB}=0.085$ is used for both the distance and the angle deviation of a HB. The strongest hydrogen bond occurs when one arm of particle (i) is co-linear with the arm of another particle (j). The size of a polar part in methanol, ethanol, propan-1-ol, and t-butanol is the same as in the 2D MB water model, i.e., $\sigma^{\rm LJ}_{\alpha\beta}=0.7r_{\rm HB}$. Sizes of all non-polar parts are $0.7r_{\rm HB}$, whereas for t-butanol it is $1.5r_{\rm HB}$. The LJ well depth, i.e., $\varepsilon^{\rm LJ}_{\alpha\beta}$, is set to $1/10|\varepsilon_{\rm HB}|$.

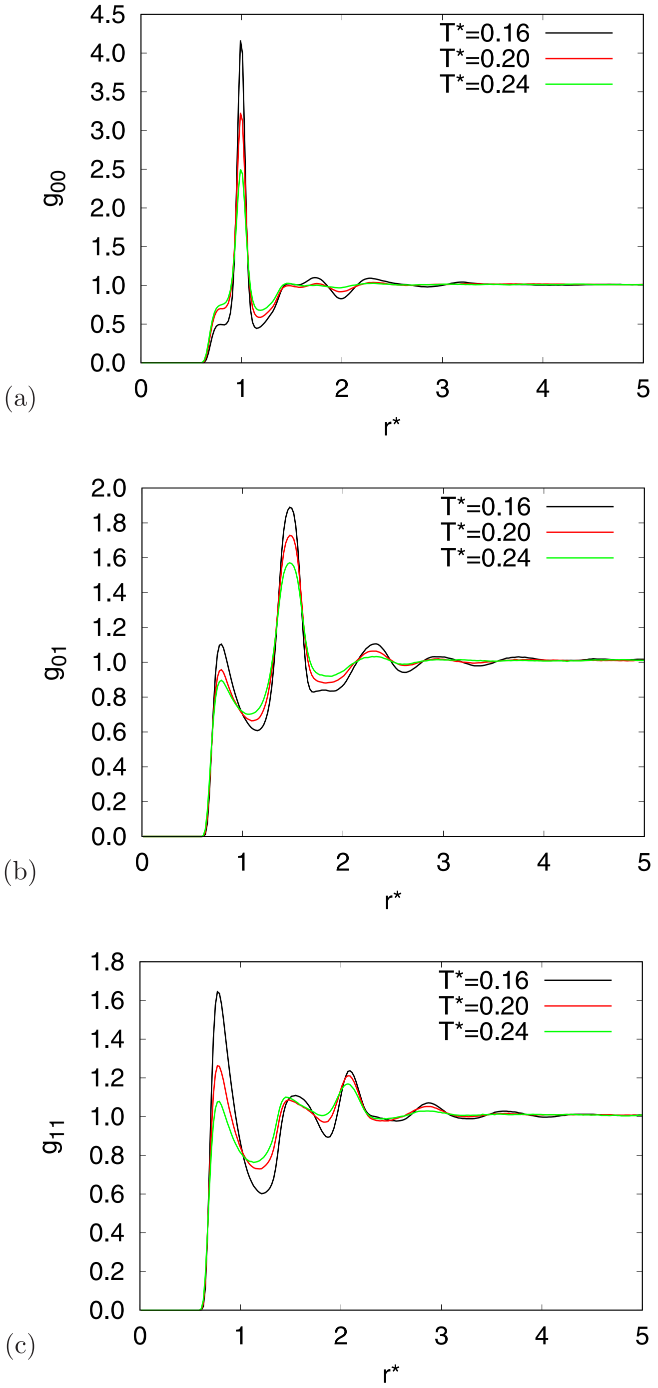

FIG. 4. Site-site pair correlation functions for methanol-like system between sites (a) 0-0, (b) 0-1, and (c) 1-1 at different temperatures.

III. MONTE CARLO SIMULATIONS

To investigate structural and thermodynamic properties of the proposed alcohol-like systems, we perform MC simulations in the NPT ensemble [50,51]. Initial configurations are constructed by inserting 100 particles randomly in a square box without overlap. Properties of the modelled alcohols are inspected in the temperature range from 0.10 to 0.50, and at pressure $p^*=0.10$. To calibrate the system, 10^4–10^6 MC

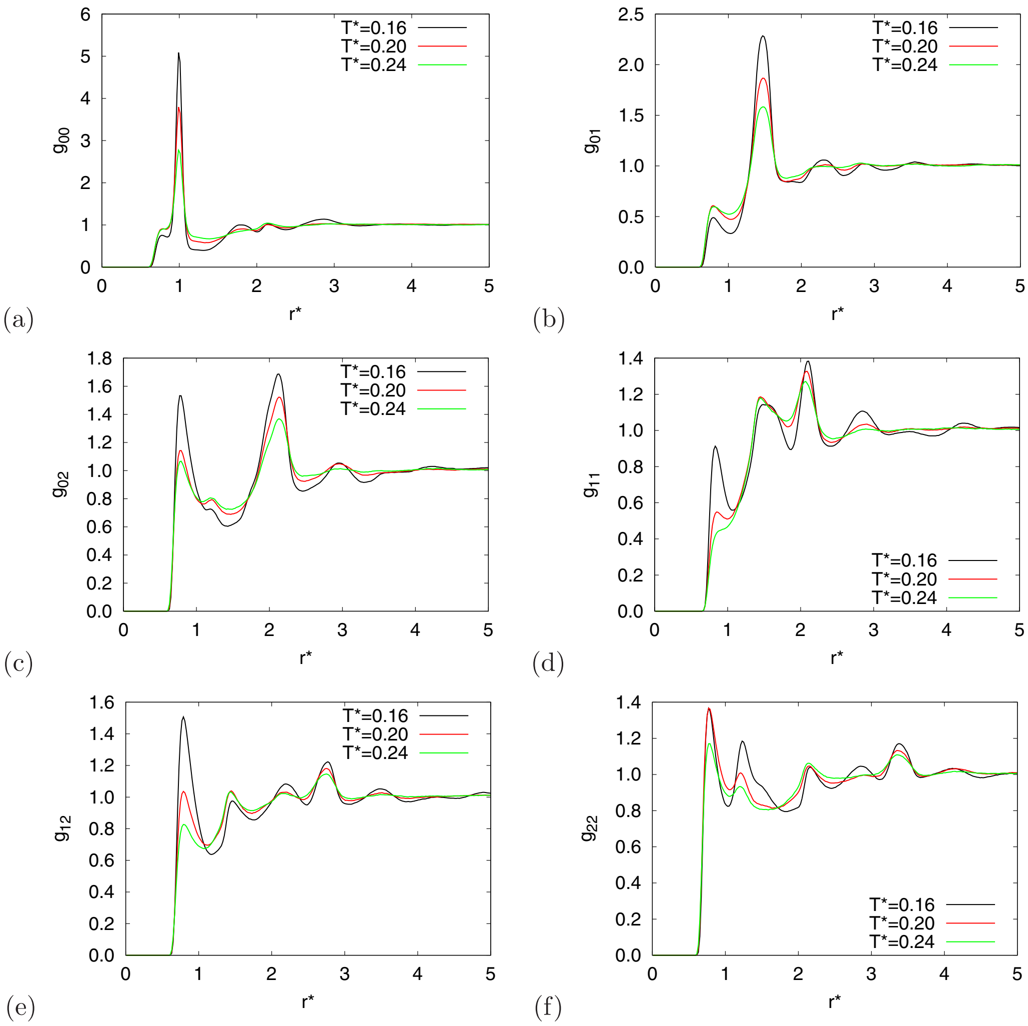

(a) (b) (c) (d) (e) (f)

FIG. 5. Site-site pair correlation functions for ethanol-like system between sites (a) 0-0, (b) 0-1, (c) 0-2, (d) 1-1, (e) 1-2, and (f) 2-2 at different temperatures.

cycles are needed and the statistics is gathered over the following 20 × 30000 MC cycles, where one cycle consists of one rotation and translation on average per particle and volume change. The cutoff potential is set to the half of the length of the simulation box. The periodic boundary conditions and minimum image convention are used to mimic the infinite system of particles.

The thermodynamic properties (heat capacity, C_P, the coefficient of isothermal compressibility, κ_T, the expansion coefficient, α) and pair distribution functions (g_{ij}) are calculated as ensemble averages [50,51]

$$C_p = \frac{\langle H^2\rangle - \langle H\rangle^2}{Nk_BT^2}, \tag{7}$$

$$\kappa_T = \frac{\langle V^2\rangle - \langle V\rangle^2}{k_BT\langle V\rangle}, \tag{8}$$

$$\alpha = \frac{\langle VH\rangle - \langle V\rangle\langle H\rangle}{k_BT^2\langle V\rangle}, \tag{9}$$

where H, V, T, k_B represent the enthalpy of the system, its volume, temperature, and Boltzmann constant, respectively.

IV. RESULTS AND DISCUSSION

All the results we show are given in reduced units. The HB energy parameter $\varepsilon_{\mathrm{HB}}$ is used to normalize temperature and enthalpy ($T^* = \frac{k_B * T}{|\varepsilon_{\mathrm{HB}}|}$, $H^* = \frac{H}{|\varepsilon_{\mathrm{HB}}|}$), while distances are normalized by the characteristic length of the hydrogen bond r_{HB} ($r^* = \frac{r}{r_{\mathrm{HB}}}$).

A. Radial distribution functions

We begin with a visual inspection of snapshots for different systems with alcohol-like properties at two different temperatures, i.e., 0.16 and 0.24, and depict them in Figs. 2 and 3. Both figures show typical structure of alcohols at lower and higher temperatures. Formed HBs are depicted with red lines.

We continue with the examination of the site-site correlation functions of modelled alcohols at three different temperatures (i.e., 0.16, 0.20, and 0.24) and show them in Figs. 4–7. Intense peaks at a distance of 1 in Figs. 4(a), 5(a), 6(a), and 7(a) indicate the formation of HBs between sites 0, which represent the hydroxyl groups. Moreover, as the

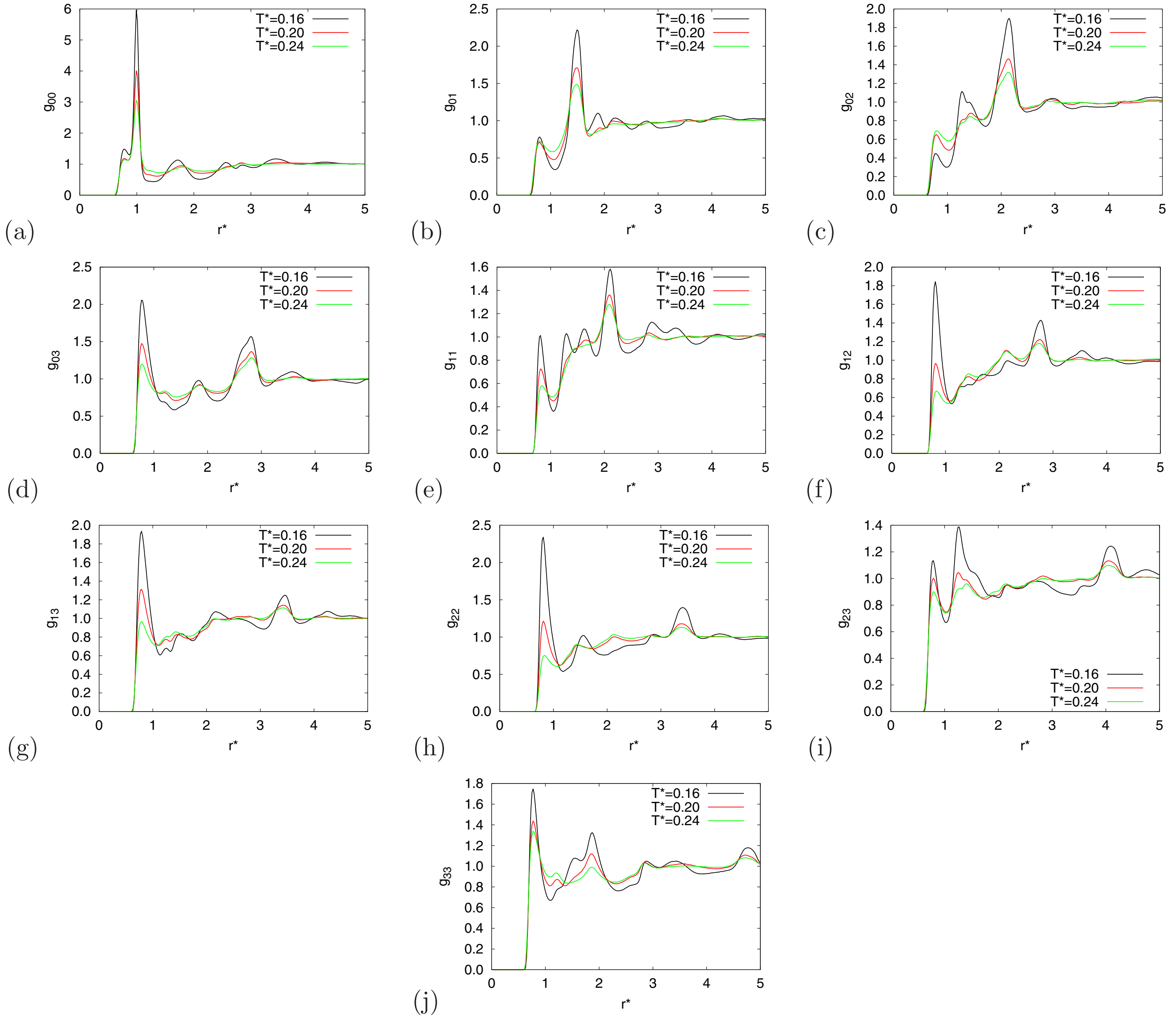

FIG. 6. Site-site pair correlation functions for propan-1-ol-like system between sites (a) 0-0, (b) 0-1, (c) 0-2, (d) 0-3, (e) 1-1, (f) 1-2, (g) 1-3, (h) 2-2, (i) 2-3, and (j) 3-3 at different temperatures.

temperature increases, the peak corresponding to the formation of HB decreases. For example, at temperature 0.24, it is approx. twice as low as that at temperature 0.16. Similar was observed for the MB water [23]. In addition, a comparison of the site-site correlation functions between polar sites displays that the strongest HB is formed in the *t*-butanol-like system, whereas the weakest HB is found in the methanol-like system (see Fig. 8). Also other peaks are observed to decrease with increasing temperature, which leads us to the conclusion that the structure with increasing temperature becomes more short ranged. The position of peaks and the width of the LJ site-site correlation functions also depend on the structure of an alcohol. In some cases, different sites are most likely to be found at a distance that corresponds to the LJ contact between them. In general, this stands for the non-polar sites located at the end of the alkyl chain of particles with alcohol-like properties [for example, see Figs. 4(c), 5(f), 6(h), 6(j), and 7(c)].

B. Hydrogen bond formation

Afterwards, we analyze the formation of HBs within systems of the alcohol-like particles. The ratio of non-HB particles and particles that form one, two, or three HBs is calculated as a function of temperature and shown in Fig. 9. As evident from Fig. 9, at the lowest temperature, i.e., 0.10, approximately 25% of particles in the methanol-like system is linked by one HB, while approximately 75% of particles form two HBs. The number of non-HB particles and particles that form three (or more) HBs is negligible (note that it is possible that one arm can form two HBs, but the energy is not favorable in comparison to one HB). On the other hand, in ethanol- and *t*-butanol-like system, which behave very similarly, approximately 40% of particles form one HB and approximately 55% two HBs. The percentage of the ethanol- and *t*-butanol- like particles that do not form any HB is small. Furthermore, at a temperature of 0.16 the ratio of particles that form two HBs

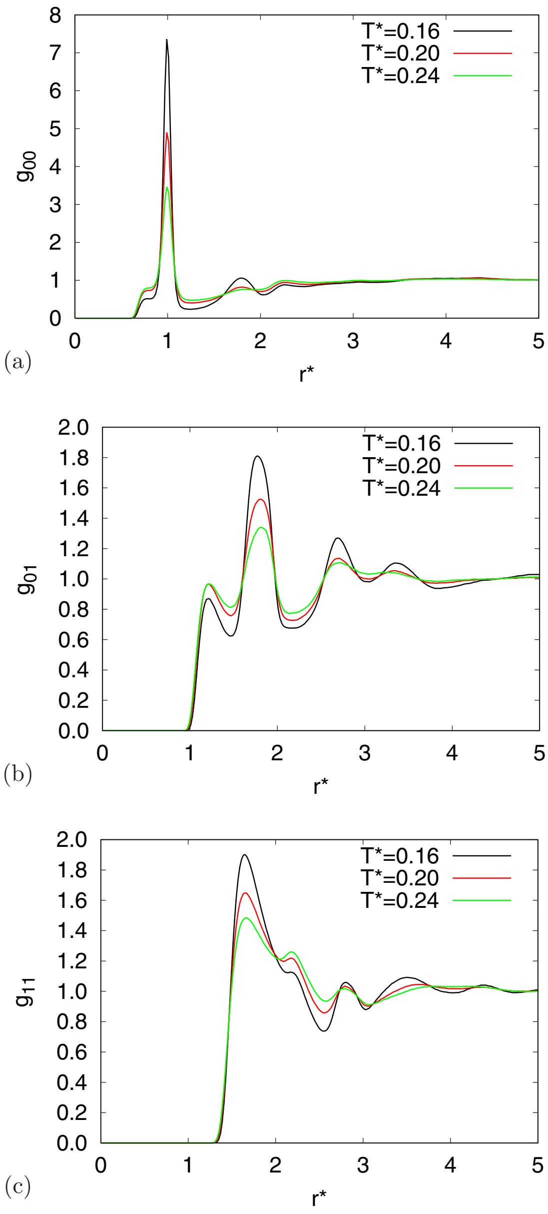

FIG. 7. Same as in Fig. 4 but for *t*-butanol-like system.

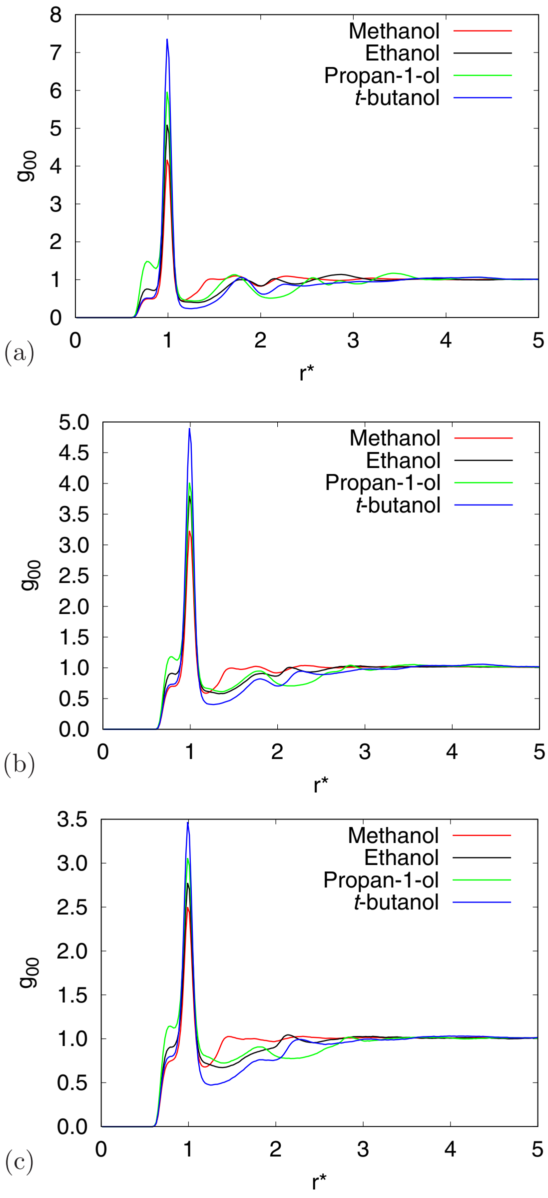

FIG. 8. Site-site pair correlation functions between sites 0-0 at temperatures (a) 0.16, (b) 0.20, and (c) 0.24 for different alcohol-like systems.

starts to decrease, while the ratio of particles linked by one HB first increases, reaches maximum at the temperature around 0.20, and afterwards starts to decrease, indicating that HBs started to melt. At a temperature of 0.24, approximately half of the particles do not form any HBs, whereas approximately 40% of particles form one HB and only 10% of particles is linked by two HBs. As shown in Fig. 9, with increasing temperature the ratio of particles linked through one, two, or three HBs decreases and at the highest temperature, i.e., 0.50, only 10% of particles form one HB, while the remaining 90% are with no HBs. Interested in the average number of formed HBs as a function of temperature, we compute them and depict in Fig. 10. We can see that we have a crossover at the temperature approximately 0.17. For populations of the once bonded particles we have inversion of order. At lower temperatures the methanol has lowest ration while at higher highest. As evident, at the lowest temperature, i.e., 0.10, the most HBs (approximately 1.7) is formed in the methanol-like system, while in the propan-1-ol-like system, the least HBs are formed. Based on the observation, we can conclude that the bigger non-polar part is attached to the hydroxyl group, the less favourable is the HB formation which is different then see for small three-dimensional (3D) alcohols, but we should stress out that HB energy is the same for all models while our quantum chemical calculations showed that t-butanol has HB energy about 30% stronger for dimer in vacuum in comparison to methanol. Additionally, the average number of HBs decreases with increasing temperature, indicating that clusters assembled of two or more particles are most likely to be found at lower temperatures, whereas smaller clusters or individual particles are expected to be present at higher temperatures. This is not in line with 3D alcohols, but in our model we have

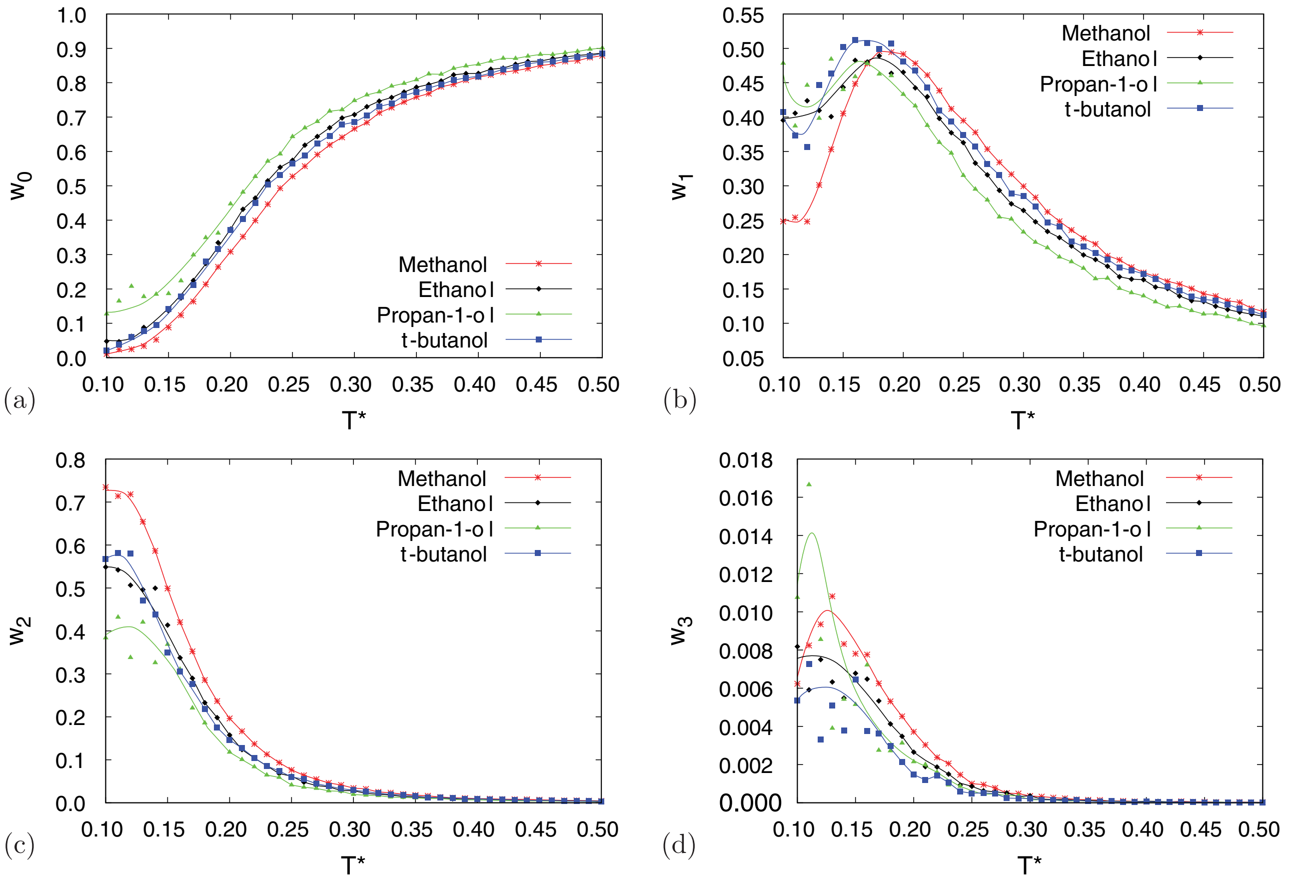

FIG. 9. Ratios of alcohol-like particles connected through different number of formed HBs [(a) 0 HB, (b) 1 HB, (c) 2 HB, (d) 3 HB] as a function of temperature.

same HB interaction so we can see only effect of non-polar part to formation of HB network.

C. Structure and analysis of the cluster size distribution

We proceed with the cluster size distribution analysis of modelled alcohols. In Fig. 11 we plot the probability of finding a particle with the alcohol-like properties in a cluster of different sizes. In the system with methanol-like properties, individual particles are most likely to be found at higher temperatures [see Figs. 11(b) and 3(c)], while at lower temperature the probability of finding an alcohol particle is similar for clusters of the size up to 6 [see Fig. 11(b)] and the tendency of forming ring-shaped structures is also observed [see Fig. 11(a)]. Similar trends are observed for all other modelled alcohols at higher temperatures, while at lower temperatures there is a lower probability of finding larger clusters of alcohol-like particles with bigger non-polar parts. In this work, ethanol-like particles associated with HBs that form a U-shape structure [see Fig. 2(b)], as suggested by Sarkar and Joarder [11] and Benmore and Loh [12], are observed. In the propan-1-ol-like system, many longer chains are present at lower temperature [see Fig. 2(c)], while at higher temperature only a few shorter chains are observed [see Fig. 3(c)]. Similar applies to the t-butanol-like system. Based on the obtained results, we suggest that the size of formed clusters depends not only on the examined system with alcohol-like properties (see Fig. 11), but also on the temperature. As can be seen from Fig. 12, the cluster size monotonically decreases with increasing temperature.

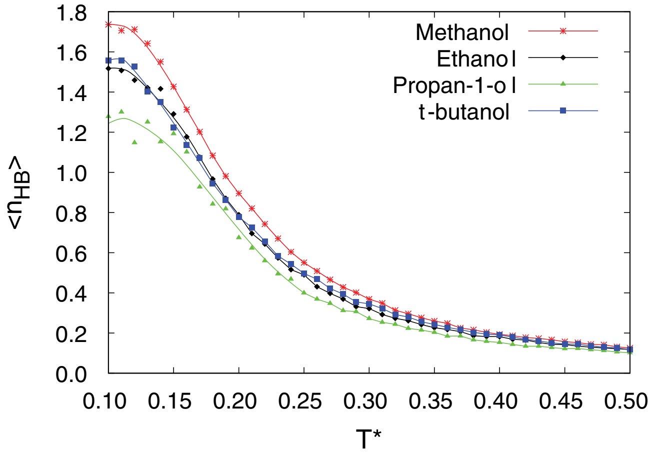

FIG. 10. The average number of formed HBs per alcohol-like particles as a function of temperature.

D. Thermodynamics

Finally, we comment on the computed temperature dependence of the density, ρ^*, the isothermal compressibility, κ^*,

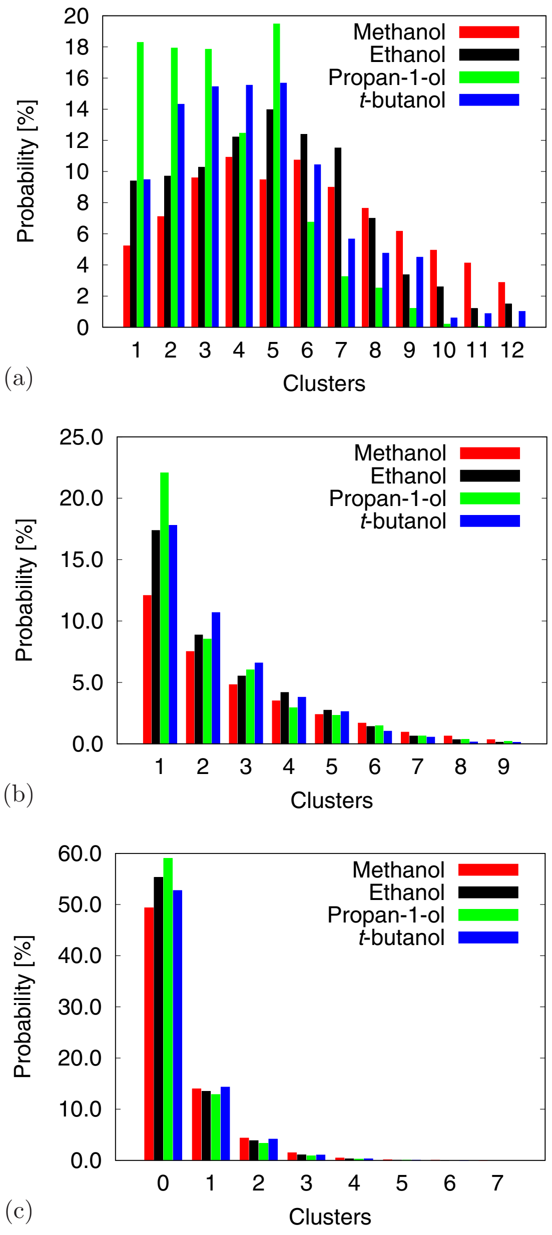

FIG. 11. Analysis of the cluster size distribution at temperatures (a) 0.14, (b) 0.16, and (c) 0.24 for different systems of particles with alcohol-like properties.

the thermal expansion coefficient, α^*, and the heat capacity, C_p^*, for different alcohol models. As shown in Fig. 13(a) the density of the alcohol-like particles monotonically decreases with increasing temperature. Methanol-like system is observed to have the highest density, as it has the smallest volume occupied by one molecule. In general, the density of particles with alcohol-like properties decreases with increasing volume of individual particle. Similar trends can be observed for all thermodynamic quantities. In addition, observed trends are comparable with the experimentally obtained data [49].

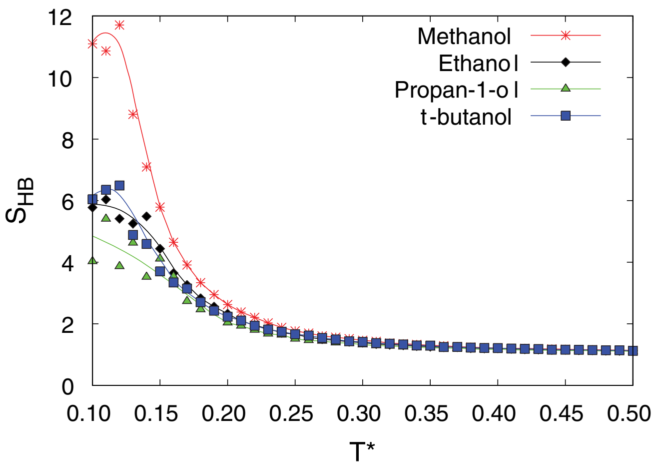

FIG. 12. Average cluster sizes as a function of temperature for different systems of alcohol-like particles.

V. CONCLUSIONS

In this study, we constructed simple 2D MB models of alcohols based on the 2D MB water model. Particles with alcohol-like properties are modelled as dimers, trimers, or tetramers of LJ disks at a fixed separation. The first LJ disk represents the hydroyxl group, while for every C atom in the alcohol's chain, another LJ disk is added. The models were assessed by MC simulations in the NPT ensemble. We computed structural and thermodynamic properties. Our results show that the HB is formed between sites that characterize alcohol's hydroxyl group, and that the position and peaks of the site-site correlation functions depend on both the alcohol structure and temperature. Similar was also observed by analyzing the cluster size distribution. We show that the average number of formed HBs between alcohol-like particles and the cluster size decreases with increasing temperature. Thermodynamic functions as functions of temperature have normal behavior as in experiments.

To conclude, the proposed simple models of lower alcohols enables us to study structure of simple organic solutes, the formation of HBs and clusters, and are able to correctly reproduce thermodynamic trends observed by experiments.

ACKNOWLEDGMENTS

We acknowledge the financial support of the Slovenian Research Agency through Grant P1-0201 as well as to projects no. J7-1816, J1-1708, N1-0186, and L2-3161 is acknowledged as well as National Institutes for Health RM1 Award No. RM1-GM135136.

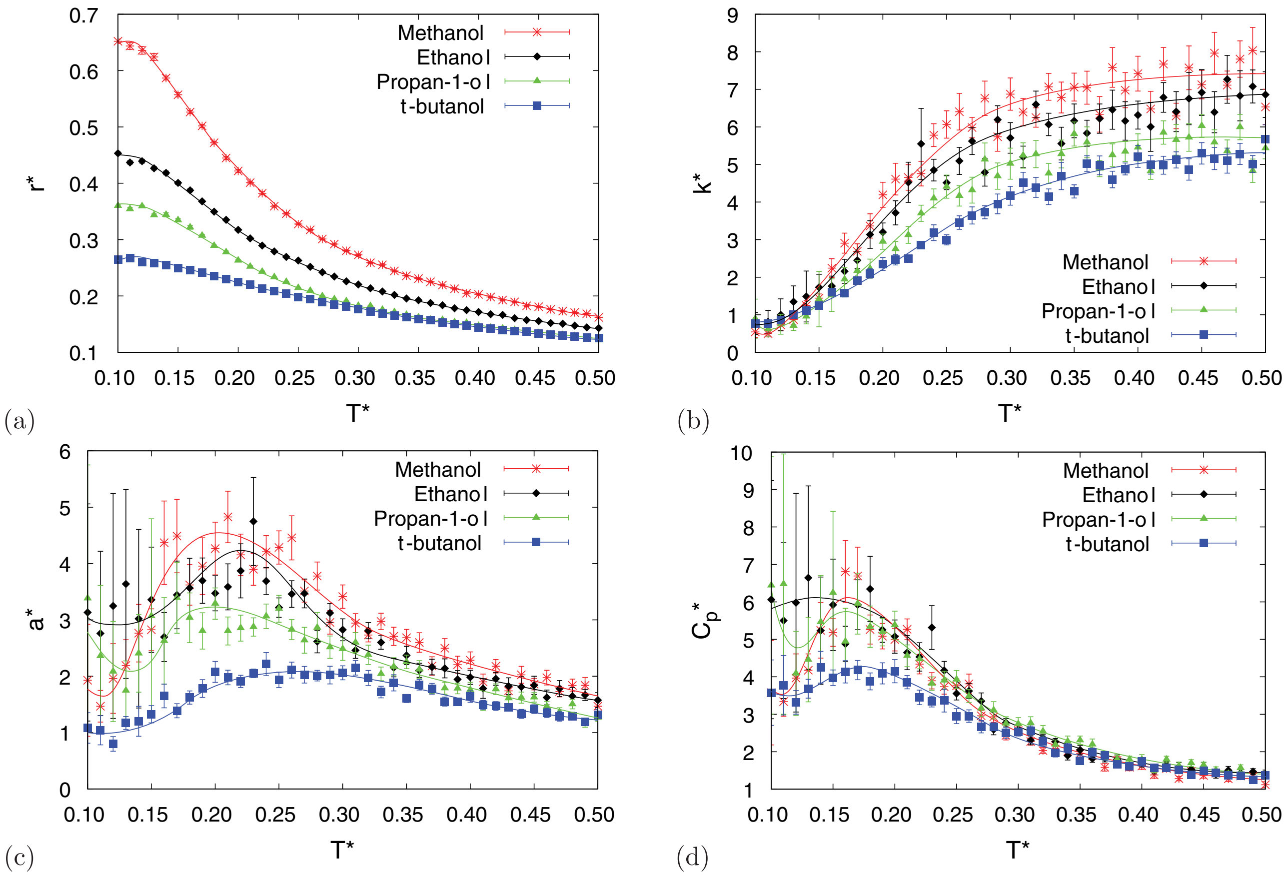

FIG. 13. Computed temperature dependence of (a) the density, (b) the isothermal compressibility, (c) the thermal expansion coefficient, and (d) the heat capacity with associated standard error, represented with error bars (with lines as a guide to the eye), for different systems with alcohol-like properties.

[1] M. Nagasaka, K. Mochizuki, V. Leloup, and N. Kosugi, J. Phys. Chem. B **118**, 4388 (2014).

[2] W. L. Jorgensen, J. Am. Chem. Soc. **102**, 543 (1980).

[3] J.-C. Soetens and P. A. Bopp, J. Phys. Chem. B **119**, 8593 (2015).

[4] A. Laaksonen, P. G. Kusalik, and I. M. Svishchev, J. Phys. Chem. A **101**, 5910 (1997).

[5] L. Pauling, *The Nature of the Chemical Bond: The Structure of Molecules and Crystals: An Introduction to Modern Structural Chemistry* (Cornell University Press, Ithaca, NY, 1960).

[6] K. Lin, X. Zhou, Y. Luo, and S. Liu, J. Phys. Chem. B **114**, 3567 (2010).

[7] S. Kashtanov, A. Augustson, J.-E. Rubensson, J. Nordgren, H. Ågren, J.-H. Guo and Y. Luo, Phys. Rev. B **71**, 104205 (2005).

[8] S. Sarkar and R. N. Joarder, J. Chem. Phys. **99**, 2032 (1993).

[9] T. Yamaguchi, K. Hidaka, and A. K. Soper, Mol. Phys. **96**, 1159 (1999).

[10] T.-J. Lin, C.-H. Hsing, C.-M. Wei, and J.-S. Kuo, Phys. Chem. Chem. Phys. **18**, 2736 (2016).

[11] S. Sarkar and R. N. Joarder, J. Chem. Phys. **100**, 5118 (1994).

[12] C. J. Benmore and Y. L. Loh, J. Chem. Phys. **112**, 5877 (2000).

[13] L. Saiz, J. A. Padró and E. Guàrdia, J. Phys. Chem. B **101**, 78 (1997).

[14] T. Takamuku, H. Maruyama, K. Watanabe, and T. Yamaguchi, J. Solution Chem. **33**, 641 (2004).

[15] A. K. Sum and S. I. Sandler, J. Phys. Chem. A **104**, 1121 (2000).

[16] A. H. Narten and S. I. Sandler, J. Chem. Phys. **71**, 2069 (1979).

[17] D. T. Bowron, J. L. Finney, and A. K. Soper, Mol. Phys. **93**, 531 (1998).

[18] B. Guillot, J. Mol. Liq. **101**, 219 (2002).

[19] S. Pothoczki, I. Pethes, L. Pusztai, L. Temleitner, D. Csókás, S. Kohara, K. Ohara, and I. Bakó, J. Mol. Liq. **329**, 115592 (2002).

[20] R. Böhmer, C. Gainarua, and R. Richert, Phys. Rep. **545**, 125 (2014).

[21] M. Tomsic, A. Jamnik, G. Fritz-Popovski, O. Glatter, and L. Vlcek, J. Phys. Chem. B **111**, 1738 (2007).

[22] T. Truskett, P. G. Debenedetti, S. Sastry, and S. Torquato, J. Chem. Phys. **111**, 2647 (1999).

[23] T. Urbic, Mol. Simul. **45**, 279 (2019).

[24] K. A. Dill, T. M. Truskett, V. Vlachy, and B. Hribar-Lee, Annu. Rev. Biophys. Biomol. Struct. **34**, 173 (2005).

[25] A. Ben–Naim, J. Chem. Phys. **54**, 3682 (1971).

[26] K. A. T. Silverstein, A. D. J. Haymet, and K. A. Dill, J. Am. Chem. Soc. **120**, 3166 (1998).

[27] G. Andaloro and R. M. Sperandeo–Mineo, Eur. J. Phys. **11**, 275 (1990).

[28] K. A. T. Silverstein, K. A. Dill, and A. D. J. Haymet, Fluid Phase Equilib. **150**, 83 (1998).

[29] N. T. Southall and K. A. Dill, J. Phys. Chem. B **104**, 1326 (2000).

[30] K. A. T. Silverstein, K. A. Dill, and A. D. J. Haymet, J. Chem. Phys. **114**, 6303 (2001).
[31] B. Hribar Lee, N. T. Southall, V. Vlachy, and K. A. Dill, J. Am. Chem. Soc. **124**, 12302 (2002).
[32] C. L. Dias, T. Hynninen, T. Ala–Nissila, A. S. Foster, and M. Karttunen, J. Chem. Phys. **134**, 65106 (2011).
[33] T. Urbic, V. Vlachy, Yu. V. Kalyuzhnyi, N. T. Southall, and K. A. Dill, J. Chem. Phys. **112**, 2843 (2000).
[34] T. Urbic, V. Vlachy, Yu. V. Kalyuzhnyi, N. T. Southall, and K. A. Dill, J. Chem. Phys. **116**, 723 (2002).
[35] T. Urbic, V. Vlachy, Yu. V. Kalyuzhnyi, and K. A. Dill, J. Chem. Phys. **118**, 5516 (2003).
[36] T. Urbic, V. Vlachy, O. Pizio, and K. A. Dill, J. Mol. Liq. **112**, 71 (2004).
[37] T. Urbic, V. Vlachy, Yu. V. Kalyuzhnyi, and K. A. Dill, J. Chem. Phys. **127**, 174511 (2007).
[38] T. Urbic, V. Vlachy, Yu. V. Kalyuzhnyi and K. A. Dill, J. Chem. Phys. **127**, 174505 (2007).
[39] T. Urbic and M. F. Holovko, J. Chem. Phys. **135**, 134706 (2011).
[40] T. Urbic and K. A. Dill, J. Chem. Phys. **132**, 224507 (2010).
[41] T. Urbic, Phys. Rev. E **85**, 061503 (2012).
[42] T. Urbic, Phys. Rev. E **94**, 042126 (2016).
[43] T. Urbic, Phys. Rev. E **96**, 032122 (2017).
[44] T. Urbic and T. Mohoric, J. Chem. Phys. **146**, 094505 (2017).
[45] P. Ogrin and T. Urbic, J. Mol. Liq. **327**, 114880 (2021).
[46] P. Ogrin and T. Urbic, J. Mol. Liq. **330**, 115671 (2021).
[47] P. Ogrin and T. Urbic, J. Mol. Liq. **337**, 116453 (2021).
[48] B. Hribar and K. A. Dill, Acta Chim. Slov. **53**, 257 (2006).
[49] T. Primorac, M. Požar, F. Sokolić, L. Zoranić, and T. Urbic, J. Mol. Liq. **262**, 46 (2018).
[50] J. P. Hansen and I. R. McDonald, *Theory of Simple Liquids* (Academic, London, 1986).
[51] D. Frenkel and B. Smit, *Molecular Simulation: From Algorithms to Applications* (Academic Press, New York, 2000).